Mitochondrion 19 (2014) 375–381

Contents lists available at ScienceDirect

Mitochondrion

journal homepage: www.elsevier.com/locate/mito

The mitochondrial proteins AtHscB and AtIsu1 involved in Fe–S cluster assembly interact with the Hsp70-type chaperon AtHscA2 and modulate its catalytic activity

Laura Leaden, Maria V. Busi, Diego F. Gomez-Casati *

Centro de Estudios Fotosintéticos y Bioquímicos (CEFOBI-CONICET), Universidad Nacional de Rosario, Suipacha 531, 2000 Rosario, Argentina

ARTICLE INFO

Available online 15 November 2014

Keywords:
Hsp70-like
Fe–S clusters
Arabidopsis
Mitochondria

ABSTRACT

Arabidopsis plants contain two genes coding for mitochondrial Hsp70-type chaperon-like proteins, AtHscA1 (At4g37910) and AtHscA2 (At5g09590). Both genes are homologs of the Ssq1 gene involved in Fe–S cluster assembly in yeast. Protein–protein interaction studies showed that AtHscA2 interacts with Atlsu1 and AtHscB, two *Arabidopsis* homologs of the Isu1 protein and the Jac1 yeast co-chaperone. Moreover, this interaction could modulate the activity of AtHscA2. In the presence of a 1:5:5 molar ratio of AtHscA2:AtIsu1:AtHscB we observed an increase in the V_{max} and a decrease in the $S_{0.5}$ for ATP of AtHscA2. Furthermore, an increase of about 28-fold in the catalytic efficiency of AtHscA2 was also observed. Results suggest that AtHscA2 in cooperation with AtIsu1 and AtHscB play an important role in the regulation of the Fe–S assembly pathway in plant mitochondria.

1. Introduction

Fe–S clusters are cofactors that function in vital processes such as redox reactions, catalysis, electron transfer, sensing of iron and oxygen levels (Balk and Pilon, 2011; Lill, 2009). The process of Fe–S cluster synthesis is highly conserved in nature and is carried out by specific proteins (Balk and Lobreaux, 2005; Muhlenhoff and Lill, 2000). In eukaryotes such as *Saccharomyces cerevisiae*, humans and plants, a mitochondrial iron–sulfur cluster (ISC) assembly machinery is required for the biosynthesis of mitochondrial Fe–S proteins involved in essential cellular processes like respiration, and photosynthesis, among others (Lill and Kispal, 2000; Muhlenhoff and Lill, 2000). However, other two biosynthetic systems have been described: NIF (nitrogen fixation) system, described in azothropic bacteria (Dos Santos et al., 2004; Rubio and Ludden, 2005); and SUF (sulfur mobilization) system, described in other bacteria such as *Escherichia coli* and also in plant plastids (Balk and Pilon, 2011; Patzer and Hantke, 1999).

In the three systems, Fe–S cluster assembly is initiated by the release of sulfur from cysteine, catalyzed by a cysteine desulfurase, Nfs1, and a iron-binding protein as Fe-donor (Lill, 2009). The sulfur is transferred to a scaffold protein and reduced to sulfide where it is combined for the assembly of the Fe–S group (Balk and Lobreaux, 2005; Balk and Pilon, 2011; Johnson et al., 2005). After the formation of the mature Fe–S cluster, this is transferred to an apoprotein. This process requires additional factors, for example, several chaperones and transfer proteins such as frataxin, a protein playing a role as Fe donor in several organisms (Babcock et al., 1997; Busi and Gomez-Casati, 2012; Koutnikova et al., 1997).

Plant frataxin was recently described in *Arabidopsis* (named AtFH). We determined the importance of this protein in the biogenesis and maturation of mitochondrial Fe–S proteins and its role in heme metabolism (Busi et al., 2004, 2006; Maliandi et al., 2011). In addition, we have demonstrated that AtFH physically interacts with the mitochondrial cysteine desulfurase (AtNfs1), the first enzyme in the Fe–S biosynthetic pathway, and modulates its catalytic activity (Turowski et al., 2012). This suggest that AtFH not only would be involved in the transfer of iron for the maturation of apoproteins but also plays a crucial role in the early steps of Fe–S cluster synthesis in plants.

However, as mentioned previously, there are other proteins that participate in the route of synthesis of Fe–S groups within mitochondria. The steps involving the maturation of the cluster after its insertion into apoproteins is specifically assisted by a molecular chaperone system, comprising by Hsp70-type chaperones and its DNA-J-like co-chaperone (J-protein) (Cupp-Vickery et al., 2004; Dutkiewicz et al., 2003).

E. coli exhibit a specialized chaperone system involved in the Fe–S cluster formation, the Hsp70 (called HscA) and the J-protein (called HscB) that facilitate the Fe–S cluster delivery mechanism in an ATP-dependent manner (Markley et al., 2013; Vickery and Cupp-Vickery, 2007). Like *E. coli*, *S. cerevisiae* display a similar chaperone system: the Hsp70 Ssq1 and the J-protein Jac1, involved in the Fe–S cluster delivery, localized in the mitochondrial matrix (Vickery and Cupp-Vickery, 2007;

* Corresponding author. Tel.: +54 341 437 1955; fax: +54 341 437 0044.
E-mail address: gomezcasati@cefobi-conicet.gov.ar (D.F. Gomez-Casati).

http://dx.doi.org/10.1016/j.mito.2014.11.002
1567-7249/

Voisine et al., 2001). The striking similarities between bacterial and yeast mechanism of Fe–S cluster delivery indicate that this machinery is conserved in all eukaryotes (Lill, 2009). The chaperone HscA/Ssq1 selectively recognizes and interacts with the conserved LPPVK peptide loop of the scaffold protein IscU/Isu1 (Chandramouli and Johnson, 2006; Dutkiewicz et al., 2004; Hoff et al., 2002). The interaction between IscU/Isu1 and HscA/Ssq1 is mediated by HscB/Jac1, which recruits the scaffold protein IscU/Isu1 *via* its conserved recognition domain and guides it to the chaperone (Andrew et al., 2006; Fuezery et al., 2011; Silberg et al., 2004). HscB/Jac1 and IscU/Isu1 synergistically stimulate the ATPase activity of the Hsp70 chaperone (Dutkiewicz et al., 2003), and the ATP hydrolysis of HscA/Ssq1 leads to a conformational change of Isu1 that decrease its affinity for the Fe–S cluster and facilitates its dissociation (Dutkiewicz et al., 2003, 2006).

In *Arabidopsis*, two genes coding for mitochondrial Hsp70-type chaperons, like proteins AtHscA1 (At4g37910) and AtHscA2 (At5g09590), that probably arose by the duplication of a gene encoding a multifunctional Hsp70 protein, have been identified (Huynen et al., 2001); in addition, a Jac1 homolog was also described (AtHscB, At5g06410) (Balk and Pilon, 2011). AtHscA1 was detected at higher levels in roots of *Arabidopsis*, but the transcript levels of *AtHscA2* were too low to resolve organ specific expression, (Sung et al., 2001), indicating that AtHscA2 is less abundant than AtHscA1 (Sung et al., 2001).

Xu et al (2009) have reported that isolated AtHscB and AtIsu1 proteins can stimulate the ATPase activity of AtHscA1, suggesting that AtHscA1 plays a role in the Fe–S cluster biogenesis in mitochondria; however, the role of AtHscA2 remains to be investigated. In the present study, we report the characterization of AtHscA2. We found that AtHscB and AtIsu1 interact with AtHscA2 and this interaction modulates its ATPase activity. Our data is in agreement with a possible participation of AtHscA2 in the mitochondrial Fe–S cluster biogenesis in plants.

2. Materials and methods

2.1. Plant material and bacterial strains

Arabidopsis (var. Columbia Col-0), grown in a greenhouse, was used in these experiments. *E. coli* BL21 (DE3) strain [*E. coli* B F − *ompT hsdS* (rB − mB −) *dcm* + Tetr *gal* (DE3) *endA* Hte [*argU ileY leuW* Cam^r]] was used for protein expression. The *E. coli* cells were grown in LB medium at 37 °C containing the appropriate antibiotics.

2.2. Cloning, expression, and purification of AtHscB, AtIsu1 and AtHscA2

Total RNA extracted from *Arabidopsis* leaves was used as template for cDNA synthesis using random hexamers. The cDNA of *AtHscA2* and *AtIsu1* were amplified by PCR using *Pfu* polymerase (Promega) and the following primers: HscA2fw 5′ CATATGAAAGAGACGGCCGAAGC 3′; HscA2rv 5′ CTCGAGCTTTTTCACTTCCTCGTACTC 3′; AtIsu1fw 5′ AAACATATGCGAACCTACCATGAG 3′; and AtIsu1rv 5′ TTTCTCGAGAGCC TGTGTGG 3′ (NdeI and XhoI restriction sites are underlined in both fw and rv primers, respectively). The PCR products were digested using restriction endonucleases and cloned into pET32c vector (Novagen). The cDNA of *AtHscB* was amplified by PCR using the following primers: AtHscBfw 5′ GGGGACAAGTTTGTACAAAAAAGCAGGCTCTGTCGACTATTT TCAGATTT 3′; and AtHscBrv 5′ GGGGACCACTTTGTACAAGAAAGCTGGG TG TCATAGCTTCTTCAAAATTT 3′. The resulting PCR product of *AtHscB* was cloned into the pDONR221 vector by recombination (Gateway technology, Invitrogen). The *AtHscB* gene cloned into the Gateway entry vector was transferred by recombination into the pDEST17 plasmid using the LR Clonase reaction. The vectors encoding for *AtIsu1* and *AtHscA2* (containing a C-terminal His-tag sequence) were named pET32-LLATIsu1 and pET32-LLAtHscA2 and the vector that codes for *AtHscB* (containing a N-terminal His-tag sequence) is pGW-LLAtHscB.

Proteins without any fusion tags were generated using the following primers: AtHscBfw-NdeI 5′ AAACATATGGTCGACTATTTTCAGATT 3′; AtHscB-stoprv 5′ TTTCTCGAGTCATAGCTTCTTCAAAAT 3′; AtIsu1fw (see above); and AtIsu1-stoprv 5′ TTTCTCGAGTCAAGCCTGTGTGGT 3′ (NdeI and XhoI restriction sites are underlined in both fw and rv primers, respectively). The PCR products were digested using restriction endonucleases and cloned into pET32c vector (Novagen). Positive clones of each of the five vectors were verified by DNA sequencing and recombinant plasmids were used to transform BL21 (DE3) *E. coli* competent cells.

2.3. Expression and purification of AtHscA2, AtIsu1 and AtHscB

E. coli BL21 (DE3) cells harboring plasmids pET32-LLAtIsu1, pET32-LLAtHscA2, pGW-LLAtHscB, pET32-LLAtIsustop and pET32-LLAAtHscBstop were grown at 37 °C in LB medium containing 100 mg ml^{-1} ampicillin to an OD_{600} = 0.6. The expression of the recombinant proteins was induced by the addition of 1 mM IPTG and subsequent incubation for 6 h a 30 °C. Cells were harvested and re-suspended in 20 mM Tris–HCl, 100 mM NaCl, 20 mM imidazole and 1 mM phenylmethylsulfonyl fluoride (PMSF), pH 7.4, disrupted by sonication and centrifuged at 7000 ×*g* for 15 min at 4 °C. The supernatants of the His-tagged proteins obtained were loaded onto a HiTrap chelating column (GE Healthcare). The column was washed with buffer A containing 20 ml of 20 mM Tris–HCl, 100 mM NaCl and 20 mM imidazole, pH 7.4. The recombinant proteins were eluted by an imidazole gradient (20–500 mM) in buffer A. The presence of the enzymes was monitored in chromatography fractions by SDS-PAGE analysis. The purified enzymes were pooled and concentrated to 1 > mg/ml, aliquoted and stored at −20 °C. Under this condition, the activity of the proteins remained stable for at least 1 month. The *E. coli* extracts of the recombinant proteins without any tags were used for the pull down experiments.

2.4. ATPase assay

ATP hydrolysis assays were performed in buffer G containing 10 mM Hepes, 100 mM KCl, 2 mM $MgCl_2$ and 0.5 mM dithiothreitol (DTT), pH 8.0. Assays were carried out at 37 °C for 15 min and activity was determined by measuring the release of inorganic phosphate using a spectrophotometric method described by Lanzetta et al. (1979) with modifications (Boshoff et al., 2004). Corrections were made for non-enzymatic breakdown of ATP by running triplicate assays on ice and subtracting these from the values obtained at 37 °C. Absorbance was determined at 660 nm and values were compared with a calibration curve using KH_2PO_4 as a standard. Specific activity was determined as μmol of phosphate released per minute per mg of protein. One unit of activity is defined as the amount of enzyme catalyzing the production of 1 μmol of ADP per minute at 37 °C. All the determinations were performed at least by triplicate and the average values ± SD are reported.

2.5. Protein interaction assays

About 200 μg of the purified proteins (AtIsu1, AtHscB, and AtHscA2, alone or in combination) were incubated in buffer G containing 2 mM ATP and incubated for 10 min at 25 °C. The resulting mixture was centrifuged using low cut off filtering device (30 kDa Centricom™ tube) to remove the non-interacting proteins. The concentrated fraction and the fraction that passed through the membrane were collected and the protein contents were analyzed by SDS-PAGE followed by Coomassie staining.

Pull-down assays were carried out as described previously (Wayllace et al., 2010). Briefly, purified His_6-tagged AtHscA2 was bound to a Ni^{2+}-Sepharose high-performance resin (GE Healthcare Bio-Sciences) previously equilibrated with buffer A, followed by the incubation with about 1 mg of *E. coli* BL21 (DE3) cell extracts expressing

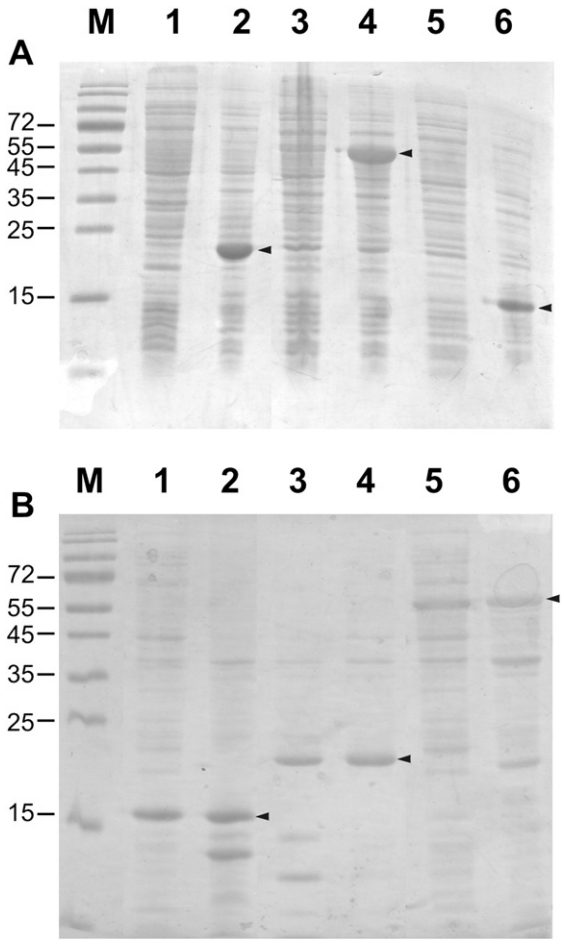

Fig. 1. Analysis of the expression of AtHscA2, AtIsu1 and AtHscB. The different *E. coli* cell extracts were electrophoresed on SDS-PAGE and stained with Coomassie Blue. (A) Total bacterial proteins containing the pGW-LLAtHscB vector before (lane 1) or after 6 h (lane 2) of added IPTG; lanes 3 and 4: total bacterial proteins containing the plasmid pET32-LLAtHscA2 before and after 6 h of added IPTG, respectively; lanes 5 and 6: total bacterial proteins containing the plasmid pET32-LLAtIsu1 before and after 6 h of added IPTG, respectively. (B) Lanes 1, 3 and 5: insoluble proteins from cells expressing AtIsu1, AtHscB and AtHscA2, respectively after 6 h of induction. Lanes 2, 4 and 6: soluble proteins from cells expressing AtIsu1, AtHscB and AtHscA2, respectively after 6 h of induction. M: Molecular mass markers (PageRuler Prestained Protein Ladder, Fermentas). Numerals on the right indicate molecular masses of the standards. Arrows indicate the protein bands corresponding to the different recombinant proteins expressed.

AtHscB or AtHscB plus AtIsu1 without tags. After washing three times with buffer A, and once with buffer containing 20 mM Tris–HCl, 50 mM NaCl, 250 mM imidazole and 1 mM phenylmethylsulfonyl fluoride (PMSF), pH 7.4, the resin was centrifuged for 3 min at 500 ×*g* and the supernatant was discarded. Bound proteins were eluted from the resin by the addition of 500 mM imidazole, and analyzed by SDS–PAGE and immunoblotting.

2.6. Additional methods

SDS-PAGE was performed using 15% P/V gels (Laemmli, 1970). Gels were developed by Coomassie Blue staining or electro-blotted onto nitrocellulose membranes (Bio-Rad). Electro-blotted membranes were incubated with a-penta-His antibody (Qiagen), a-AtHscB or a-AtIsu1. The antigen–antibody complex was visualized with alkaline phosphatase-linked a-mouse IgG or a-rabbit IgG and BCIP and NBT staining (Bollag et al., 1996). Total protein concentration was determined as described by Bradford (1976). Statistical analyses: Significant differences were determined using Student's t-test. Values statistically different from the control ($P < 0.05$) are denoted with letters in the figures.

3. Results

3.1. Cloning, expression and purification of recombinant proteins

AtHscA2, *AtHscB* and *AtIsu1* cDNA were obtained by RT-PCR using specific primers. After amplification, *AtHscA2* and *AtIsu1* were digested and cloned into the expression vector pET32c to generate pET32-LLAtHscA2 and pET32-LLATIsu1. Both reverse primers do not contain a stop codon, thus leading to the expression of a C-terminal His_6 tag sequence. The cDNA from *AtHscB* was recombined with the pDEST17 vector to generate the plasmid named pGW-LLAtHscB, which contain a N-terminal His_6-tag sequence. The expression of the three recombinant proteins was carried out in *E. coli* BL21 (DE3) cells. After the addition of IPTG, cell harvesting and SDS-PAGE analysis we observed three protein bands with apparent molecular mass of 15.9, 20.1 and 55 kDa, in agreement with the predicted molecular mass of AtIsu1, AtHscB and AtHscA2, respectively (Fig. 1A). When cells were collected, sonicated and centrifuged, about 60%, 70% and 50% of AtIsu1, AtHscB

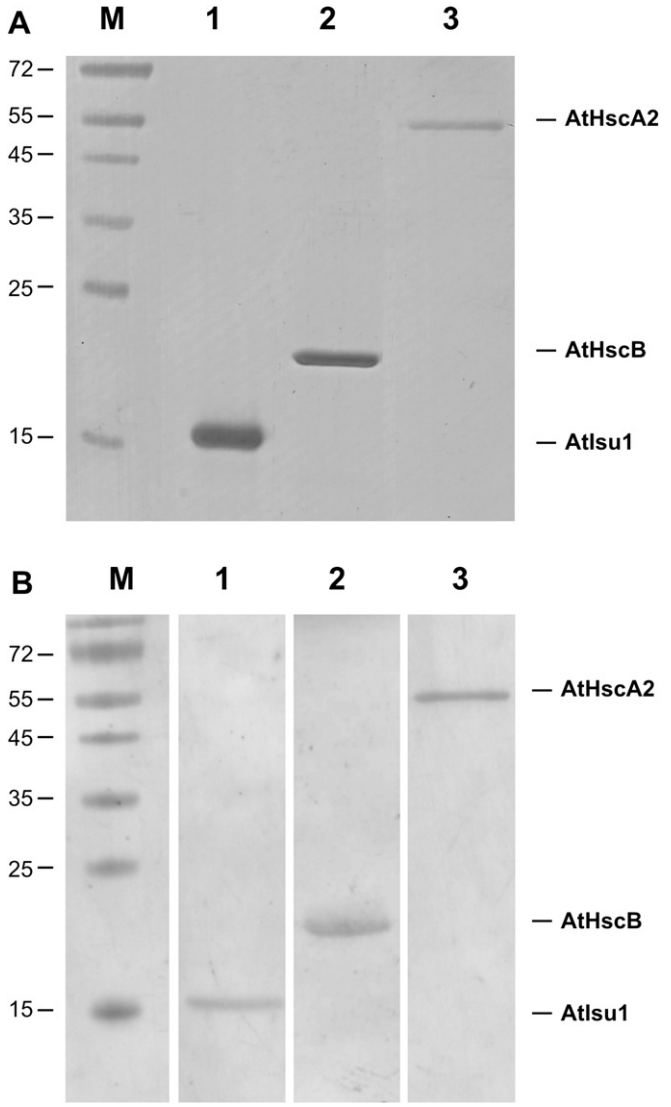

Fig. 2. SDS-PAGE and western blot analysis of the purified recombinant proteins. (A) SDS-PAGE analysis of AtIsu1 (lane 1), AtHscB (lane 2) and AtHscA2 (lane 3). (B) Western blot analysis of AtIsu1, AtHscB and AtHscA2 corresponds to lanes 1, 2 and 3, respectively. M: Molecular mass markers (PageRuler Prestained Protein Ladder, Fermentas).

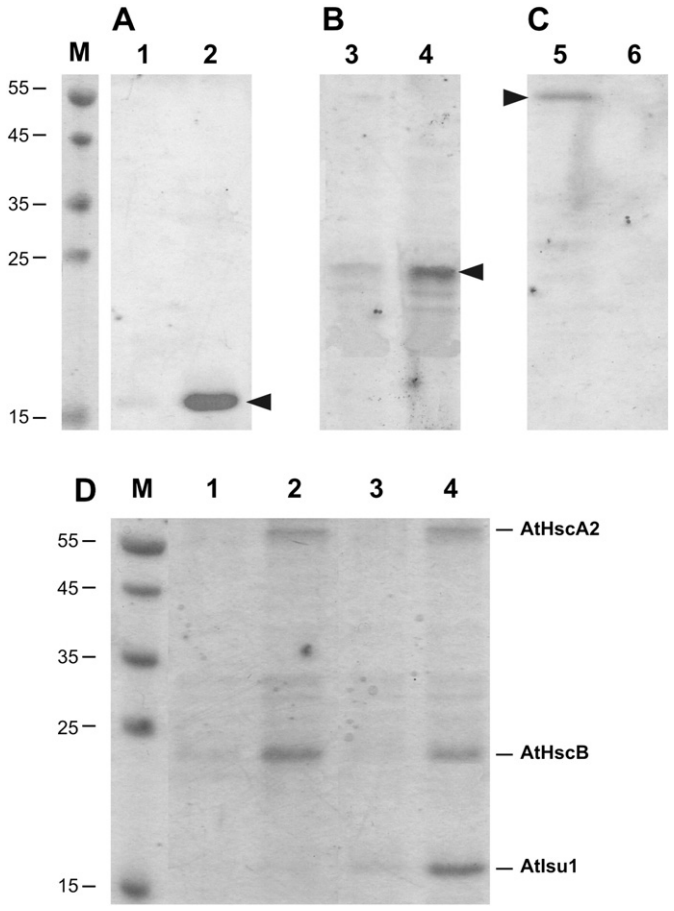

Fig. 3. SDS-PAGE analysis of protein–protein interaction assays. (A) Concentrated (lane 1) and filtered (lane 2) fractions of purified AtIsu1 after centrifugation on Centricom tubes. (B) Concentrated (lane 3) and filtered (lane 4) fractions of purified AtHscB after centrifugation using Centricom tubes. (C) Concentrated (lane 5) and filtered (lane 6) - fractions of AtHscA2 after centrifugation. (D) Filtered (lane 1) and concentrated (lane 2) fractions of AtHscA2 incubated in the presence of AtHscB. Lanes 3 and 4 correspond to the filtered and concentrated fractions, respectively, of the incubation of AtHscA2 in the presence of both, AtIsu1 and AtHscB proteins. M: Molecular mass markers (PageRuler Prestained Protein Ladder, Fermentas).

and AtHscA2, respectively, were obtained in the supernatant fraction of the homogenate (Fig. 1B). The recombinant proteins were purified using a HiTrap chelating column as described in the Materials and methods section and analyzed using SDS-PAGE (Fig. 2A), and the presence of each recombinant protein was confirmed by immunoblotting using a-His antibodies (Fig. 2B).

3.2. Interaction between AtHscA2, AtIsu1 and AtHscB

It has been reported that the J-protein AtHscB interacts with the scaffold protein AtIsu1, both in yeast-two hybrid assays and complemented a yeast Δ*jac1* mutant (Xu et al., 2009). To investigate the existence of a possible protein–protein interaction with AtHscA2, we performed *in vitro* interaction assays using two different techniques: 1) a centrifugation using a low cut off Centricom tube and 2) *in vitro* pull down assays (see the Materials and methods section).

For the centrifugation technique, AtHscB, AtIsu1 or AtHscA2 proteins were placed and centrifuged in different Centricom tubes as controls. After centrifugation, the samples contained in the top of the tube (concentrated fraction) and the samples that passed through the membrane were analyzed. The analysis on SDS-PAGE revealed, as expected, that AtHscA2 did not pass through the membrane, whereas the bulk of AtIsu1 and AtHscB was found in the fraction which was filtered through the Centricom membrane (Fig. 3A–C). When AtHscB was incubated with HscA2 in the presence of ATP, only a small amount (less than 10%) of AtHscB filtered through the membrane while more than 90% of the protein was found in the concentrated fraction with AtHscA2 (Fig. 3D), suggesting that these proteins could physically interact.

We also evaluated if AtHscB and AtIsu1 could interact with AtHscA2. After incubating the three proteins for 10 min at 25 °C, and the subsequent centrifugation in the Centricom tubes, we found that more than 90% of AtIsu1 remains with AtHscA2 and AtHscB (Fig. 3D).

To confirm the protein–protein interactions we performed pull-down assays using *E. coli* extracts expressing recombinant AtHscB and AtIsu1 without any tags and AtHscA2-His_6. After the incubation of AtHscA2-His_6 extract with the Ni^{2+} resin and AtHscB, two protein bands were observed by SDS-PAGE analysis, a 19 kDa band, corresponding to AtHscB-stop and a 55 kDa band corresponding to AtHscA2-His_6 (Fig. 4A). A third protein band of about 15 kDa corresponding to AtIsu1-stop was observed when AtIsu1 and AtHscB were incubated with the AtHscA2 bounded to the resin (lane 2, Fig. 4A). The incubation of AtHscB-stop or AtIsu1-stop extract with Ni^{2+} resin alone did not show the presence of any protein band, indicating that these interactions are specific (Fig. 4A, lanes 4 and 5). The protein bands were detected by

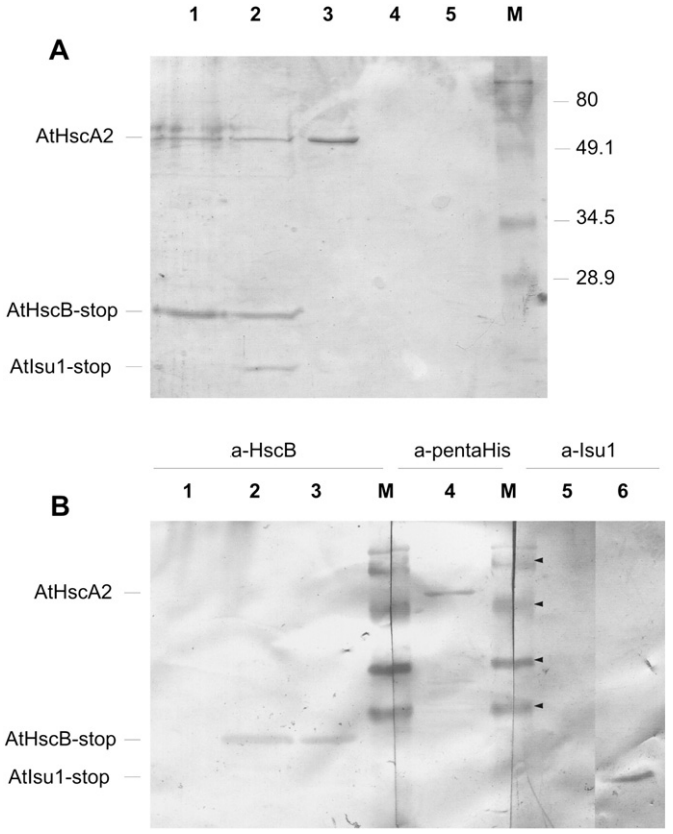

Fig. 4. SDS-PAGE and western blot analysis of pull-down technique of recombinant AtHscA2, AtIsu1 and AtHscB proteins. A) SDS-PAGE analysis; lane 1, AtHscB protein was recovered together with AtHscA2; lane 2, AtIsu1 and AtHscB proteins were recovered with AtHscA2; lane 3, shows the recovered AtHscA2 bound to Ni^{2+} resin; lanes 4 and 5, show the absence of nonspecifically binding to the resin for AtHscB (lane 4) or AtIsu1 (lane 5) (control). (B) Western blot analysis of pull-down assays. Proteins in lanes 1, 2 and 3 were identified using a-AtHscB; AtHscA2 in lane 4 was identified with a-penta-His antibodies and proteins in lanes 5 and 6, using a-Isu1 antibody. Lane 1 shows the absence of AtHscB after incubation with the Ni^{2+} resin (control); lane 2 shows the presence of AtHscB after incubation with AtIsu1 and AtHscA2 and; lane 3 shows AtHscB after incubation with AtHscA2; lane 4 shows a protein band corresponding to AtHscA2 after incubation with AtIsu1 and AHscB using a-penta-His antibodies; lane 5 shows the absence of AtIsu1 (control) after incubation with the Ni^{2+} resin; lane 6 shows the presence of AtIsu1 after incubation with AtHscA2 and AtHscB, using anti-AtIsu1. Numerals on the right indicate molecular masses of the standards (Bio-Rad prestained protein marker broad range).

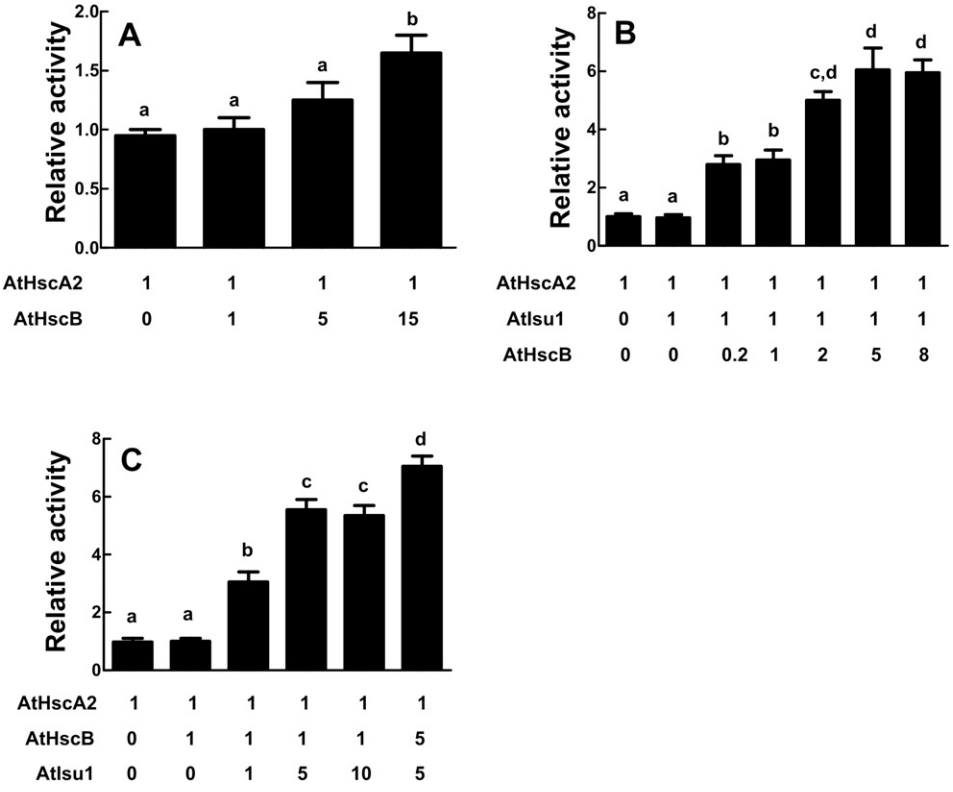

Fig. 5. Effect of AtHscB and AtIsu1 on the activity of AtHscA2. (A) Fold activation of AtHscA2 in the presence of variable molar amounts of AtHscB. (B) Fold activation of AtHscA2 in the presence of variable molar amounts of AtHscB and constant quantity of AtIsu1. (C) Fold activation of AtHscA2 in the presence of different amounts of AtHscB and AtIsu1. Values statistically different from the control ($P < 0.05$) are denoted with different letters.

western blot using a-AtHscB, a-AtIsu1 and a-penta-His antibodies (Fig. 4B). Our results suggest that the three proteins could interact forming a multiprotein complex.

3.3. Effect of AtIsu1 and AtHScB on the kinetics of AtHscA2

To evaluate if the interaction observed between AtIsu1, AtHscB and AtHscA2 has an effect on the ATPase activity of AtHscA2, we measured ATP hydrolysis in the presence and absence of AtHscB and AtIsu1, using a colorimetric assay monitoring the release of inorganic phosphate (Pi) (Lanzetta et al., 1979).

First, we measured the effect of AtHscB on the ATPase activity of AtHscA2. For this purpose, ATP hydrolysis in the presence of different concentrations of AtHscB was determined (Fig. 5A). We did not observe any significant effect at AtHscA2:AtHscB molar ratio of 1:1 and 1:5. In contrast, at 1:15 ratio we found that AtHscB increases the activity of AtHscA2 about 1.6-fold.

We decided then to study the effect of AtHscB and AtIsu1 on the activity of AtHscA2. For this purpose, we evaluated the effect of different concentrations of AtHscB when AtIsu1 remained constant (1:1 molar ratio with respect to AtHscA2). The ATPase activity of AtHscA2 was increased about 2.7 and 3.0-fold at AtHscA2:AtIsu1:AtHscB molar ratio of 1:1:0.2 and 1:1:1, respectively (Fig. 5B). Moreover, in the presence of 2, 5 or 8–fold higher concentration of AtHscB, the activity of AtHscA2 was increased about 5.0, 6.1 and 6.0-fold, respectively (Fig. 5B).

When AtHscB concentration remains constant (1:1 molar ratio with respect to AtHscA2), we observed about 3.1, 5.5 and 5.4-fold activation of AtHscA2 at 1:1:1, 1:1:5 and 1:1:10 AtHscA2:AtHscB:AtIsu1 molar ratio, respectively (Fig. 5C). Taken together, our results suggest that AtISu1 and AtHscB could modulate the AtHscA2 activity in a cooperative manner.

Thus, we determined the kinetic parameters for ATP of AtHscA2 alone and in the presence of different molar ratios of AtHscB and AtIsu1 (Table 1 and Fig. 6). The $S_{0.5}$ and V_{max} of AtHscA2 are 38 ± 3 and 7.3 ± 0.8, respectively. Results show that in the presence of 1:1:1 molar ratio of AtHscA2:AtIsu1:AtHscB, there is not a significant variation in the apparent affinity for ATP, whereas about 2.9-fold increase in the V_{max} was observed and a 2.6-fold increase in the catalytic efficiency was observed (Fig. 6, Table 1). In the presence of 1:5:5 molar ratio of the above proteins, we found a 3.2-fold decrease in the $S_{0.5}$ (see Figs. 5 and 6), whereas about 8.8-fold increase in the V_{max} with respect to that obtained with AtHscA2 alone was observed. In addition, results show a 28-fold increase in the catalytic efficiency under this condition.

4. Discussion

The insertion of a Fe–S cluster into an apoprotein is a complex process where several scaffold proteins interact with a molecular chaperone system to assemble these inorganic groups (Schilke et al., 2006). At the present, little is known about the chaperones and scaffold proteins involved in this pathway in plant mitochondria. In *S. cerevisiae* it was reported that two mitochondrial Hsp70s, Ssc1 and its paralogue Ssq1, function together with the J-protein Jac1 to assist the biogenesis of the Fe–S centers, being Ssq1 1000-fold less abundant than Ssc1 (Dutkiewicz et al., 2003).

Ssc1 is a multifunctional mitochondrial Hsp70 involved in different processes including translocation across the mitochondrial inner membrane, folding of proteins after the import and reactivation or degradation of proteins after exposure to stress, while the Ssq1 protein plays a specific role in the assembly of the Fe–S clusters: it was described that Isu1, the scaffold protein where the Fe–S groups are assembled, is the substrate Ssq1, whereas the co-chaperone Jac1 stabilizes the interaction between Isu1 and Ssq1 (Andrew et al., 2006;

Table 1
Kinetic parameters for the substrate ATP of AtHscA2.

	$S_{0.5}$ (μM)	n_H	V_{max} (mU/mg)	$V_{max}/S_{0.5}$
AtHscA2	38 ± 3	0.9 ± 0.2	7.3 ± 0.8	0.19 ± 0.04
AtHscA2:AtIsu1:AtHscB (1:1:1)[a]	42 ± 4	1.1 ± 0.2	21.3 ± 1.6	0.50 ± 0.08
AtHscA2:AtIsu1:AtHscB (1:5:5)[a]	12 ± 2	1.0 ± 0.1	64.2 ± 4.3	5.33 ± 1.25

[a] Molar ratio.

Dutkiewicz et al., 2003). Ssq1 is present only in a few fungal species. In all other eukaryotes the generic mitochondrial Hsp70 performs this function in Fe–S cluster formation in addition to its roles in mitochondrial protein import and folding (Lill et al., 2012; Uhrigshardt et al., 2010). This hypothesis is supported by the finding that in *S. cerevisiae* when the specialized Ssq1 is knocked out, Ssc1 can participate in Fe–S cluster biosynthesis, but less efficiently since the participation of Jac1 is needed to stimulate the ATPase activity of Ssq1 (Voisine et al., 2001). On the other hand, it has been reported that mtHSP70 chaperone is the only Hsp70 present in human mitochondria (Cai et al., 2013; Rouault, 2012). It has been demonstrated that mtHsp70 interact with Hsc20 (Jac1 homolog) and both proteins have an important role in the synthesis of Fe–S clusters in human mitochondria (Shan and Cortopassi, 2012).

Arabidopsis plants have two mitochondrial Hsp70s proteins, AtHscA1 and AtHscA2, showing 48% and 51% of identity, respectively, compared to yeast Ssq1 (Huynen et al., 2001; Schilke et al., 2006). These proteins are mitochondrial chaperones that arose by the duplication of a gene encoding a multifunctional Hsp70 and they have 80% of identity between them. In addition, it has been described that AtHscA1 can functionally complement a Δ*ssq1* yeast mutant (Xu et al., 2009), suggesting that at least AtHscA1 could play a function in the iron sulfur cluster biogenesis in plants (Huynen et al., 2001). As mentioned previously for Ssq1, *AtHscA2* transcript is less abundant than the *AtHscA1* mRNA (Sung et al., 2001), suggesting that like mitochondrial chaperones of *S. cerevisiae*, AtHscA1 and AtHscA2 could play different roles in plants.

Xu et al. (2009) also reported that AtHscB can interact with AtIsu1. This result is in agreement with the interaction found between their yeast counterparts, Jac1/Isu1 (Ciesielski et al., 2012; Dutkiewicz et al., 2003). Taken together, these data suggest that the Jac1/Isu1 and the AtHscB/AtIsu1 interaction play an important role in the mitochondrial Fe–S cluster biogenesis.

With the aim to characterize the second *Arabidopsis* Hsp70 protein, AtHscA2, we evaluate the possible interaction with AtIsu1 and AtHscB. Our results show that AtHscB and AtHscA2 could physically interact *in vitro*. In addition, we found that the three proteins, AtHscB, AtHscA2 and AtIsu1 could also physically interact. This data is in agreement with the yeast model where Jac1 recruits the scaffold protein Isu1 *via* its conserved recognition domain and this complex can be targeted to the chaperone (Andrew et al., 2006; Dutkiewicz et al., 2006; Fuezery et al., 2011; Silberg et al., 2004).

Due to the finding that AtHscB and AtIsu1 can interact with AtHscA2, we further analyze whether this interaction could modulate the ATPase activity of AtHscA2.

We observed that AtHscB alone (AtHscA2:AtHscB molar ratio up to 1:5) has no effect on the AtHscA2 activity, whereas a 1:15 molar ratio of AtHscA2:AtHscB was able to activate the ATP hydrolysis about 1.6-fold. In the same way, when AtIsu1 alone was present in the reaction mix, the ATPase activity of AtHscA2 was not significantly activated. However, in the presence of AtHscA2, AtIsu1 and AtHscB proteins at a 1:1:1 molar ratio, we observed about 3-fold activation; whereas the highest activation of the ATP hydrolysis of AtHscA2 was observed when the molar quantities of AtIsu1 and AtHscB were both 5-fold higher with respect to AtHscA2, suggesting that AtHscB and AtIsu1 cooperatively modulate the AtHscA2 catalytic activity. Moreover, the ATP hydrolysis of AtHscA2 was activated 2.7-fold, when the molar ratio of AtHscA2:AtIsu1:AtHscB was 1:1:0.2, indicating the relevance of the AtIsu1 in the modulation of the AtHscA2 catalytic activity.

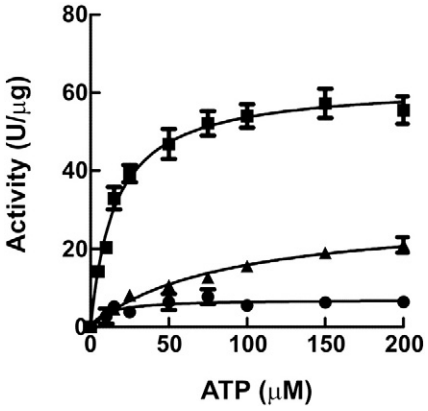

Fig. 6. ATP saturation plots for AtHscA2. Assays were performed with 0.5 μM of AtHscA2 alone (circles) or in the presence of 1:1:1 (triangles) or 1:5:5 (squares) molar amount of AtHscA2:AtIsu1:AtHscB.

In the presence of AtHscA2 alone, we observed a $S_{0.5}$ close to that reported for AtHscA1 (Xu et al., 2009), whereas in the presence of AtHscA2:AtIsu1:AtHscB (1:5:5 molar ratio) we observed a 3.2-fold decrease in the $S_{0.5}$ value and almost a 28-fold increase in the catalytic efficiency for AtHscA2. Taken together, these results suggest that AtIsu1 and AtHscB have an important role in regulating the ATPase activity of AtHscA2.

As mentioned above, it has been reported that in *E. coli* and *S. cerevisiae*, the chaperones involved in Fe–S cluster formation HscA/Ssq1 undergoes an ATP-dependent-hydrolysis, highly specific interaction with the LPPVK motif of Isu1 dependent of HscB/Jac1 (Cupp-Vickery et al., 2004; Dutkiewicz et al., 2004; Hoff et al., 2003; Schilke et al., 2006). The energy derived from the ATP hydrolysis induces a structural change in Isu1, facilitating cluster dissociation and transfer to apoproteins (Chandramouli and Johnson, 2006; Dutkiewicz et al., 2004; Lill, 2009). We found that AtIsu1 contains the conserved LPPVK motif between the residues 130 and 136, suggesting that it could play a similar role in the interaction with AtHscA2. On the other hand, AtHscB can functionally replace yeast Jac1 and interacts with AtIsu1 (Xu et al., 2009) and AtIsu1 can complement Δ*isu1* yeasts (Leon et al., 2005; Tone et al., 2004). Moreover, mutant plants deficient in AtHscB have reduced activity of at least two Fe–S proteins such as aconitase and succinate dehydrogenase activities, all of this suggest that AtHscB and AtIsu1 are involved in the Fe–S cluster biogenesis.

5. Conclusion

In agreement with the data reported for *S. cerevisiae*, our data show the interaction among AtIsu1, AtHscB and AtHscA2. Moreover we found that this interaction modulates the AtHscA2 catalytic activity. Taken together, these results suggest that not only AtHscA1 but also AtHscA2 in cooperation with AtIsu1 and AtHscB could play a role in the Fe–S cluster formation in plant mitochondria.

Acknowledgments

This work was supported by grants from ANPCyT (PICT 0512 and 2188). LL is a Doctoral fellow from CONICET. MVB and DGC are research members from CONICET.

References

Andrew, A.J., Dutkiewicz, R., Knieszner, H., Craig, E.A., Marszalek, J., 2006. Characterization of the interaction between the J-protein Jac1p and the scaffold for Fe–S cluster biogenesis, Isu1p. J. Biol. Chem. 281, 14580–14587.

Babcock, M., de Silva, D., Oaks, R., Davis-Kaplan, S., Jiralerspong, S., Montermini, L., Pandolfo, M., Kaplan, J., 1997. Regulation of mitochondrial iron accumulation by Yfh1p, a putative homolog of frataxin. Science 276, 1709–1712.
Balk, J., Lobreaux, S., 2005. Biogenesis of iron–sulfur proteins in plants. Trends Plant Sci. 10, 324–331.
Balk, J., Pilon, M., 2011. Ancient and essential: the assembly of iron–sulfur clusters in plants. Trends Plant Sci. 16, 218–226.
Bollag, D.M., Rozycki, M.D., Edelstein, S.J., 1996. Protein Methods, 2nd ed. Wiley-Liss, New York.
Boshoff, A., Hennessy, F., Blatch, G.L., 2004. The in vivo and in vitro characterization of DnaK from *Agrobacterium tumefaciens* RUOR. Protein Expr. Purif. 38, 161–169.
Bradford, M.M., 1976. A rapid and sensitive method for the quantitation of microgram quantities of protein utilizing the principle of protein–dye binding. Anal. Biochem. 248–254.
Busi, M.V., Gomez-Casati, D.F., 2012. Exploring frataxin function. IUBMB Life 64, 56–63.
Busi, M.V., Zabaleta, E.J., Araya, A., Gomez-Casati, D.F., 2004. Functional and molecular characterization of the frataxin homolog from *Arabidopsis thaliana*. FEBS Lett. 576, 141–144.
Busi, M.V., Maliandi, M.V., Valdez, H., Clemente, M., Zabaleta, E.J., Araya, A., Gomez-Casati, D.F., 2006. Deficiency of *Arabidopsis thaliana* frataxin alters activity of mitochondrial Fe–S proteins and induces oxidative stress. Plant J. 48, 873–882.
Cai, K., Frederick, R.O., Kim, J.H., Reinen, N.M., Tonelli, M., Markley, J.L., 2013. Human mitochondrial chaperone (mtHSP70) and cysteine desulfurase (NFS1) bind preferentially to the disordered conformation, whereas co-chaperone (HSC20) binds to the structured conformation of the iron–sulfur cluster scaffold protein (ISCU). J. Biol. Chem. 288, 28755–28770.
Chandramouli, K., Johnson, M.K., 2006. HscA and HscB stimulate [2Fe–2S] cluster transfer from IscU to apoferredoxin in an ATP-dependent reaction. Biochemistry 45, 11087–11095.
Ciesielski, S.J., Schilke, B.A., Osipiuk, J., Bigelow, L., Mulligan, R., Majewska, J., Joachimiak, A., Marszalek, J., Craig, E.A., Dutkiewicz, R., 2012. Interaction of J-protein co-chaperone Jac1 with Fe–S scaffold Isu is indispensable in vivo and conserved in evolution. J. Mol. Biol. 417, 1–12.
Cupp-Vickery, J.R., Peterson, J.C., Ta, D.T., Vickery, L.E., 2004. Crystal structure of the molecular chaperone HscA substrate binding domain complexed with the IscU recognition peptide ELPPVKIHC. J. Mol. Biol. 342, 1265–1278.
Dos Santos, P.C., Dean, D.R., Hu, Y., Ribbe, M.W., 2004. Formation and insertion of the nitrogenase iron–molybdenum cofactor. Chem. Rev. 104, 1159–1173.
Dutkiewicz, R., Schilke, B., Knieszner, H., Walter, W., Craig, E.A., Marszalek, J., 2003. Ssq1, a mitochondrial Hsp70 involved in iron–sulfur (Fe/S) center biogenesis. Similarities to and differences from its bacterial counterpart. J. Biol. Chem. 278, 29719–29727.
Dutkiewicz, R., Schilke, B., Cheng, S., Knieszner, H., Craig, E.A., Marszalek, J., 2004. Sequence-specific interaction between mitochondrial Fe–S scaffold protein Isu and Hsp70 Ssq1 is essential for their in vivo function. J. Biol. Chem. 279, 29167–29174.
Dutkiewicz, R., Marszalek, J., Schilke, B., Craig, E.A., Lill, R., Muhlenhoff, U., 2006. The Hsp70 chaperone Ssq1p is dispensable for iron–sulfur cluster formation on the scaffold protein Isu1p. J. Biol. Chem. 281, 7801–7808.
Fuezery, A.K., Oh, J.J., Ta, D.T., Vickery, L.E., Markley, J.L., 2011. Three hydrophobic amino acids in *Escherichia coli* HscB make the greatest contribution to the stability of the HscB–IscU complex. BMC Biochem. 12, 3.
Hoff, K.G., Ta, D.T., Tapley, T.L., Silberg, J.J., Vickery, L.E., 2002. Hsc66 substrate specificity is directed toward a discrete region of the iron–sulfur cluster template protein IscU. J. Biol. Chem. 277, 27353–27359.
Hoff, K.G., Cupp-Vickery, J.R., Vickery, L.E., 2003. Contributions of the LPPVK motif of the iron–sulfur template protein IscU to interactions with the Hsc66–Hsc20 chaperone system. J. Biol. Chem. 278, 37582–37589.
Huynen, M.A., Snel, B., Bork, P., Gibson, T.J., 2001. The phylogenetic distribution of frataxin indicates a role in iron–sulfur cluster protein assembly. Hum. Mol. Genet. 10, 2463–2468.
Johnson, D.C., Dean, D.R., Smith, A.D., Johnson, M.K., 2005. Structure, function, and formation of biological iron–sulfur clusters. Annu. Rev. Biochem. 74, 247–281.
Koutnikova, H., Campuzano, V., Foury, F., Dolle, P., Cazzalini, O., Koenig, M., 1997. Studies of human, mouse and yeast homologues indicate a mitochondrial function for frataxin. Nat. Genet. 16, 345–351.
Laemmli, U.K., 1970. Cleavage of structural proteins during the assembly of the head of bacteriophage T4. Nature 227, 680–685.
Lanzetta, P.A., Alvarez, L.J., Reinach, P.S., Candia, O.A., 1979. An improved assay for nanomole amounts of inorganic phosphate. Anal. Biochem. 100, 95–97.
Leon, S., Touraine, B., Briat, J.F., Lobreaux, S., 2005. Mitochondrial localization of *Arabidopsis thaliana* Isu Fe–S scaffold proteins. FEBS Lett. 579, 1930–1934.
Lill, R., 2009. Function and biogenesis of iron–sulphur proteins. Nature 460, 831–838.
Lill, R., Kispal, G., 2000. Maturation of cellular Fe–S proteins: an essential function of mitochondria. Trends Biochem. Sci. 25, 352–356.
Lill, R., Hoffmann, B., Molik, S., Pierik, A.J., Rietzschel, N., Stehling, O., Uzarska, M.A., Webert, H., Wilbrecht, C., Muhlenhoff, U., 2012. The role of mitochondria in cellular iron–sulfur protein biogenesis and iron metabolism. Biochim. Biophys. Acta 1823, 1491–1508.
Maliandi, M.V., Busi, M.V., Turowski, V.R., Leaden, L., Araya, A., Gomez-Casati, D.F., 2011. The mitochondrial protein frataxin is essential for heme biosynthesis in plants. FEBS J. 278, 470–481.
Markley, J.L., Kim, J.H., Dai, Z., Bothe, J.R., Cai, K., Frederick, R.O., Tonelli, M., 2013. Metamorphic protein IscU alternates conformations in the course of its role as the scaffold protein for iron–sulfur cluster biosynthesis and delivery. FEBS Lett. 587, 1172–1179.
Muhlenhoff, U., Lill, R., 2000. Biogenesis of iron–sulfur proteins in eukaryotes: a novel task of mitochondria that is inherited from bacteria. Biochim. Biophys. Acta 1459, 370–382.
Patzer, S.I., Hantke, K., 1999. SufS is a NifS-like protein, and SufD is necessary for stability of the [2Fe–2S] FhuF protein in *Escherichia coli*. J. Bacteriol. 181, 3307–3309.
Rouault, T.A., 2012. Biogenesis of iron–sulfur clusters in mammalian cells: new insights and relevance to human disease. Dis. Model Mech. 5, 155–164.
Rubio, L.M., Ludden, P.W., 2005. Maturation of nitrogenase: a biochemical puzzle. J. Bacteriol. 187, 405–414.
Schilke, B., Williams, B., Knieszner, H., Pukszta, S., D'Silva, P., Craig, E.A., Marszalek, J., 2006. Evolution of mitochondrial chaperones utilized in Fe–S cluster biogenesis. Curr. Biol. 16, 1660–1665.
Shan, Y., Cortopassi, G., 2012. HSC20 interacts with frataxin and is involved in iron–sulfur cluster biogenesis and iron homeostasis. Hum. Mol. Genet. 21, 1457–1469.
Silberg, J.J., Tapley, T.L., Hoff, K.G., Vickery, L.E., 2004. Regulation of the HscA ATPase reaction cycle by the co-chaperone HscB and the iron–sulfur cluster assembly protein IscU. J. Biol. Chem. 279, 53924–53931.
Sung, D.Y., Vierling, E., Guy, C.L., 2001. Comprehensive expression profile analysis of the *Arabidopsis* Hsp70 gene family. Plant Physiol. 126, 789–800.
Tone, Y., Kawai-Yamada, M., Uchimiya, H., 2004. Isolation and characterization of *Arabidopsis thaliana* ISU1 gene. Biochim. Biophys. Acta 1680, 171–175.
Turowski, V.R., Busi, M.V., Gomez-Casati, D.F., 2012. Structural and functional studies of the mitochondrial cysteine desulfurase from *Arabidopsis thaliana*. Mol. Plant 5, 1001–1010.
Uhrigshardt, H., Singh, A., Kovtunovych, G., Ghosh, M., Rouault, T.A., 2010. Characterization of the human HSC20, an unusual DnaJ type III protein, involved in iron–sulfur cluster biogenesis. Hum. Mol. Genet. 19, 3816–3834.
Vickery, L.E., Cupp-Vickery, J.R., 2007. Molecular chaperones HscA/Ssq1 and HscB/Jac1 and their roles in iron–sulfur protein maturation. Crit. Rev. Biochem. Mol. Biol. 42, 95–111.
Voisine, C., Cheng, Y.C., Ohlson, M., Schilke, B., Hoff, K., Beinert, H., Marszalek, J., Craig, E.A., 2001. Jac1, a mitochondrial J-type chaperone, is involved in the biogenesis of Fe/S clusters in *Saccharomyces cerevisiae*. Proc. Natl. Acad. Sci. U. S. A. 98, 1483–1488.
Wayllace, N.Z., Valdez, H.A., Ugalde, R.A., Busi, M.V., Gomez-Casati, D.F., 2010. The starch-binding capacity of the noncatalytic SBD2 region and the interaction between the N- and C-terminal domains are involved in the modulation of the activity of starch synthase III from *Arabidopsis thaliana*. FEBS J. 277, 428–440.
Xu, X.M., Lin, H., Latijnhouwers, M., Moller, S.G., 2009. Dual localized AtHscB involved in iron sulfur protein biogenesis in *Arabidopsis*. PLoS ONE 4, e7662.